Bunzkögele

(Thomas J. Sausgruber, Alexander Preh & Rainer Poisel)

Modified after the paper by Sausgruber J.Th., Preh A. & Poisel R. (2010): Bunzkoegele south slope – a complex failure mechanism shaped by sliding of joints and breaking of rock. –Mitteilungen für Ingenieurgeologie und Geomechanik, 9: 1-14. Wien

WGS coordinates: 47°01´43.15´´ N , 12° 33´49.82´´ E
Site, county: Matrei, Eastern Tyrol
Type of the slope failure: deep-seated rockslide
Volume: 1km^3
Age: postglacial

The Bunzkögele Mountain exhibits a deep seated ancient landslide in the vicinity of Matrei, Eastern Tyrol, Austria. A high mountain relief characterizes the location. The area of investigation is surrounded by deep morphological structures, which were particularly formed by the last Ice Age and subsequent fluvial processes, representing the Tauern Valley to the west and the Bretterwand Canyon to the east and to the south. The maximum elevation difference from the summit of Bunzkögele to the Bretterwand Canyon is 1.160 m (Fig. 1). In the deep N-S running Bretterwand Canyon the base of the landslide is exposed, showing a maximum depth of 350 m. The volume of the landslide is approximately 1 km³.

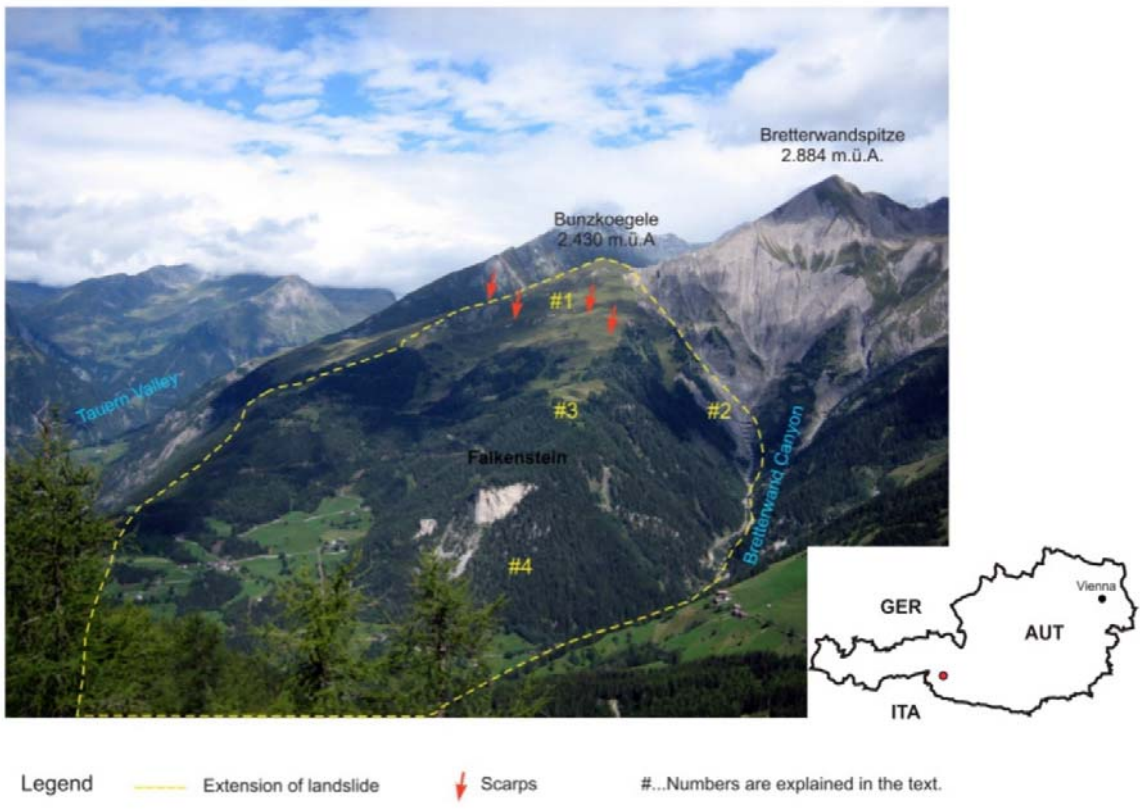

Figure 1. Landslide Bunzkoegele

Geological and structural setting

The landslide is situated on the southern rim of the tectonic Tauern Window, where two major tectonic units after STAUB (1924) and CORNELIUS & CLAR (1939) can be specified:

1. Matrei Zone and
2. Glockner Nappe.

The rocks of the Glockner Nappe show a thick sequence of metamorphic shales, marls and limestones including fragments of oceanic lithosphere, which were deposited in the former Penninic Ocean in Cretaceous times (Fig. 2). The Alpine orogeny caused these sediments to be intensively folded and faulted. Several geological units have been detached and stacked, producing a voluminous orogenic wedge (LAMMERER & WEGER 1998). The Matrei Zone represents the old suture zone, where the Penninic Ocean was subducted. It is therefore extremely strained and has the character of a melange zone including several allochthonous rock slices from the neighbouring Austroalpine shelf margin (PESTAL ET AL. 2009), e.g. the dolomite marble crag of Falkenstein (Fig. 1 and Fig. 2). The collision of the European and the Adriatic plate cumulated in early Tertiary, affecting the sediments by a regional metamorphism reaching the amphibolit facies in the centre of the window and the greenschist facies in the outer zones (FRANK ET AL. 1987). Continuing N-S compression combined with E-W extension led to the exhumation of the inner Tauern Window, i.e. Penninic Nappes during the Oligocene and Miocen (SELVERSTONE 1988).

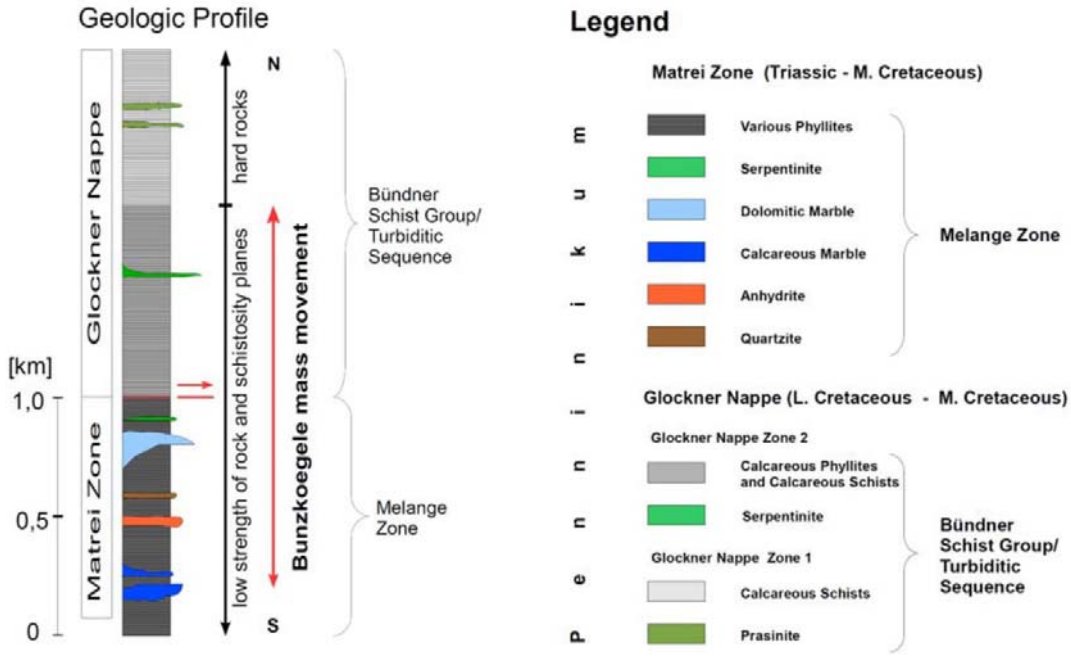

Figure 3. Geologic profile

Geomorphologic and structural features of the landslide

The Bunzkögele Mountain shows some unique geomorphologic features, which characterize the area as a deep seated landslide. Besides that, the north-south running Bretterwand Canyon presents the rare outcrop situation, where one can observe the internal deformation. By mapping the landslide, three different parts may be distinguished:

a) Head of the landslide (regions # 1 and # 2)

On top of the mountain several big scarps are encountered to form a big staircase (Fig. 3a). They follow the schistosity, which dips 60° to the south (Fig. 3b). The maximum vertical offset at the main scarp (1) reaches 70 m. In the Bretterwand Canyon, where the internal deformation of the landslide is exposed, the originally parallel, south dipping rock lamellae are deformed to an S-structure by

slope tectonics. Fig. 4a shows the upper hinge of the kink-band fold. The lower one cannot be seen in the Fig. but it is exposed at two localities in the deepest parts of the canyon.

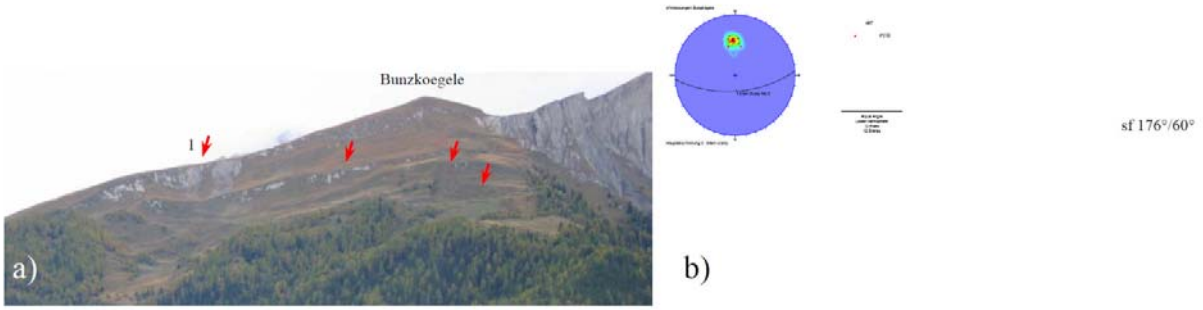

Figure 3 a) Region # 1, main scarps b) Contour plot of schistosity planes from the main scarp no.1 (stereographic projection of poles and main great circle)

Figure 4. Region # 2, Hinge zone and Contour plot of schistosity planes; reconstruction of fold axis (stereographic projection of poles and main great circles)

b) Middle part of the landslide (region # 3)
Here some obvious trenches can be observed (Fig. 5a). The schistosity planes are nearly vertically (Fig. 5b).

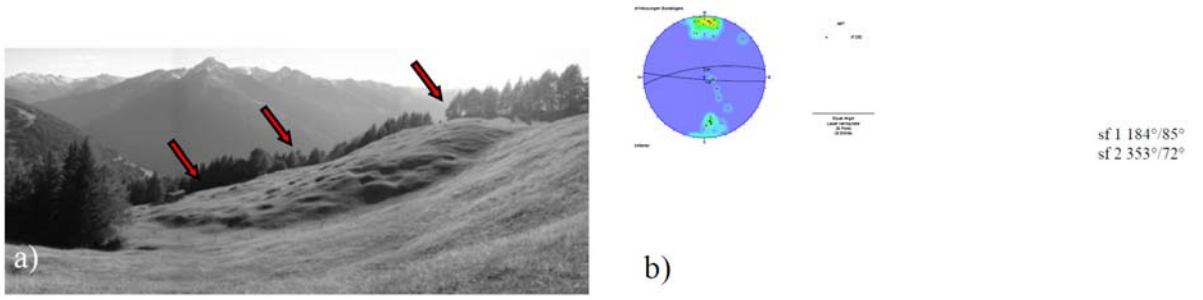

Figure 5. Region # 3 a) Trenches b) Contour plot of schistosity planes (stereographic projection of poles and main great circles)

c) Toe of the landslide (region # 4)
In this part the rock lamellae are overturned and the morphology is sawtooth like stepped (Fig. 6a). These features result from flexural toppling. The schistosity planes dip 20° to north east (Fig. 6b).

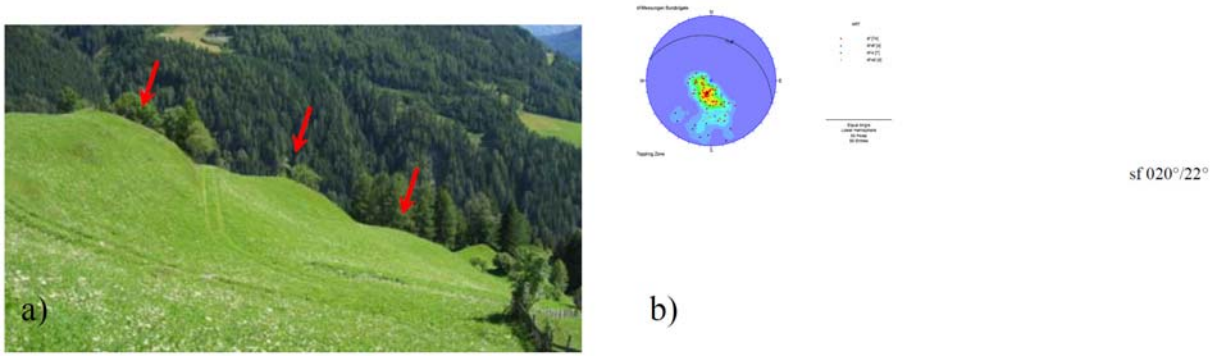

Figure 6. Region # 4 a) Sawtooth morphology b) Contour plot of schistosity planes (stereographic projection of poles and main great circle)

State of research
A profound mechanical explanation of the landslide was given by ZISCHINSKY (1966, 1969), who studied the locality in the 60s. He used CLAR's approach (CLAR 1963, CLAR & WEISS 1965) to work out the deformation pattern of the rock lamellae from slope tectonics (Fig. 7). If one assumes a constant and uniform deformation over time, as ZISCHINSKY (1966, 1969) has done, the lines of deformation gives rise to the velocities. The velocity distribution in the middle part of the mass movement offers Fig. 7 on the right hand side. Therein the highest velocity occurs at the top, which diminishes to zero at the base of the landslide. This specific velocity distribution was in accordance with ZISCHINSKY's (1966) startling discovery in the field, where no distinct basal shear zone exists. Therefore he idealised the rock mass by a continuum and viscous deformation. ZISCHINSKY (1966, 1969) called this type of mass movement "Sackung", in English sagging. In contrast to a "Sackung", slide shows more or less an equal velocity distribution from top to base.

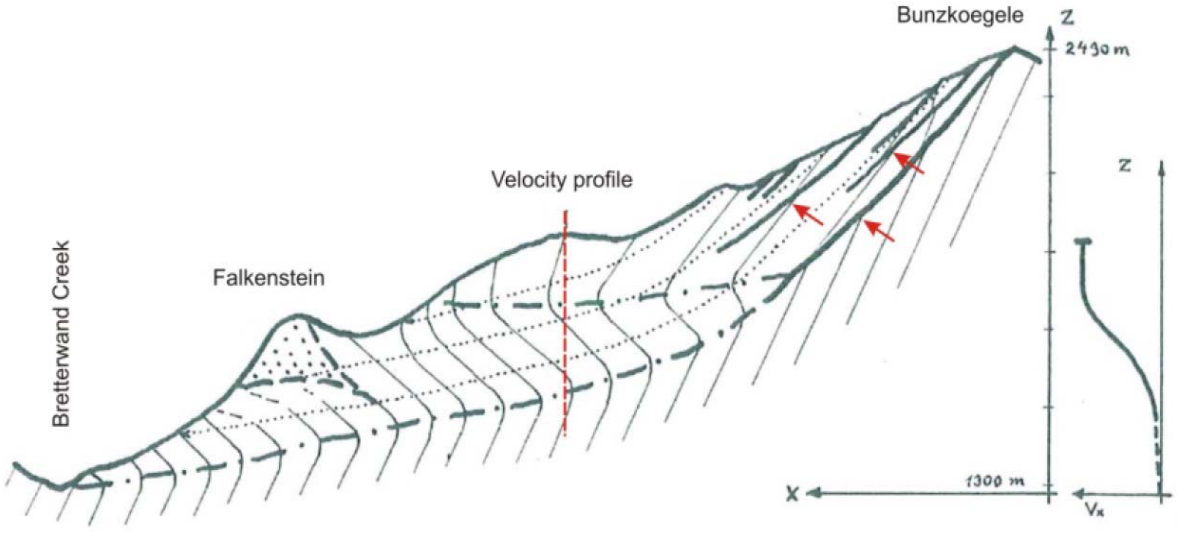

Figure 7. Cross section of the landslide from ZISCHINSKY (1966, 1969), slightly modified

Reinvestigation of the site

To model the failure behaviour of the landslide with a numerical program, a reinvestigation of the site has been carried out. This included the mapping of morphological structures, structural geologic features concerning slope tectonics and the collection of geotechnical properties of the rock mass involved in the landslide process.

Rock mass properties

The UCS (Uniaxial Compressive Strength) was determined by the ISRM field method (ISRM 1981b). For estimating the GSI (Geological Strength Index) the table for flysch sediments from MARINOS & HOEK (2001) was applied. The discontinuities of interest, which are the schistosity planes, were assessed descriptively, by visual inspection from ISRM (1981a).

Concerning Table 1 the rock mass of Bunzkoegele south slope is characterized by low strength. The phyllites display smooth and undulating schistosity planes. Hard rock slices of marble and quartzite, which occur in the Matrei Zone (Fig. 2), have limited extensions. Thus they do not alter the general mechanical properties. Within the Gockner Nappe zone 2 the rock mass properties reflect the nature of the turbiditc metasediments. The sequence includes mainly calcareous phyllites with occasional intercalations of calcareous schists. Even so the properties are better than those in the Matrei Zone, the Glockner Nappe zone 2 still being characterised by its low strength. Additionally graphitic phyllites are common in the whole sequence, which have an extremely low friction. They play an important role for the failure mechanism. E.g. they were mapped at the main scarps, so one can assume that they initiated normal faulting of the rock lamellae at the head of the slope.

Area	rock	UCS [MPa]	Roughness of schistosity planes	GSI
Matrei Zone	various phyllites; often graphitic phyllites	5-25	slickensided / undulating	10-30 H-G
Glockner Nappe zone 2	mainly calcareous phyllite, intercalations of calcareous schists a. graphitic phyllite	5-100	slickensided / undulating occasionally rough / undulating	20-30 (30-40) G-E (D-C)
Glockner Nappe zone 1	calcareous schists and marble	100-150	rough / undulating - planar	40-50 B

Table 1. Geomechanical properties of rocks and schistosity planes

Mechanic analysis

The mechanics of the landslide is explained by Fig.8, which is a reinterpretation of ZISCHINSKY's (1966, 1969) cross section (Fig. 7). The specific structure of the rock mass is given by the 60° southward dipping schistosity representing a relative constant structural element at the southern border of the Tauern Window. This was idealised by a raster of parallel rock lamellae. To get the shape of the lamellae, which was formed by slope tectonics, the measurements of the schistosity planes were projected onto the cross section. The kinematic was gained by a restoration of the deformed structures as well as by kinematic indicators mapped in the outcrops.

The failure starts by normal faulting at the head of the mountain, which leads to the formation of scarps. At the same time the rock lamellae are deformed in an S-shape manner. A short north dipping limb occurs between two long south dipping limbs, forming a kink-band fold. The hinges are relatively sharp (Fig. 4). An important finding in the field is the lack of distinct basal gliding surface. With reference to ZISCHINSKY'S (1966, 1969) cross section, the normal faults do not cut through the raster of the rock lamellae, but they simply use the given planes of weakness, which are the schistosity planes.

A result of the formation of the kink-band fold is, that

a) the vectors of movement change their inclination of dip, from steep 60° to flat 15° southward dipping (s. Fig. 15) and

b) the lamellae rotate.

The rotation of the lamellae is clockwise up to an angle of 15° for those in the upper part (lamellae no. 1 to 4). Within the kink-band they rotate counter clockwise up to an angle of 65°. A specific role during deformation is played by the development of antithetic faults. For kinematic reasons they are indispensable and allow the slumped rock mass to move further on. The reason for antithetic faults to form is due to the described change in the steepness of dip of the displacement vectors (MANDL 1988). During movement of the mass a successive mobilisation of newly formed antithetic faults is going on. They emanate where the shear zone has a sharp bend and the displacement vectors have a kink (Fig. 15). Occasionally some synthetic faults develop due to simple shear between two normal faults, which are the schistosity planes (Fig. 9).

In the middle section of the landslide the S-structure of the rock lamellae (no. 5-8) is still present. In contrast to its upper part, however, the schistosity planes near the surface rotate counter clockwise, from the originally southward inclination to an overturned northward one. The lamellae fan out causing tensile failure to occur. Several mapped trenches, which strike parallel to the schistosty, indicate an area of dilation (Fig. 5).

At the toe's area the S-structure disappears and only a flexural toppling can be recognised. The rock lamellae (no. 9-15) bend counter clockwise to a maximum angle of 100° (Fig. 6 and Fig. 8).

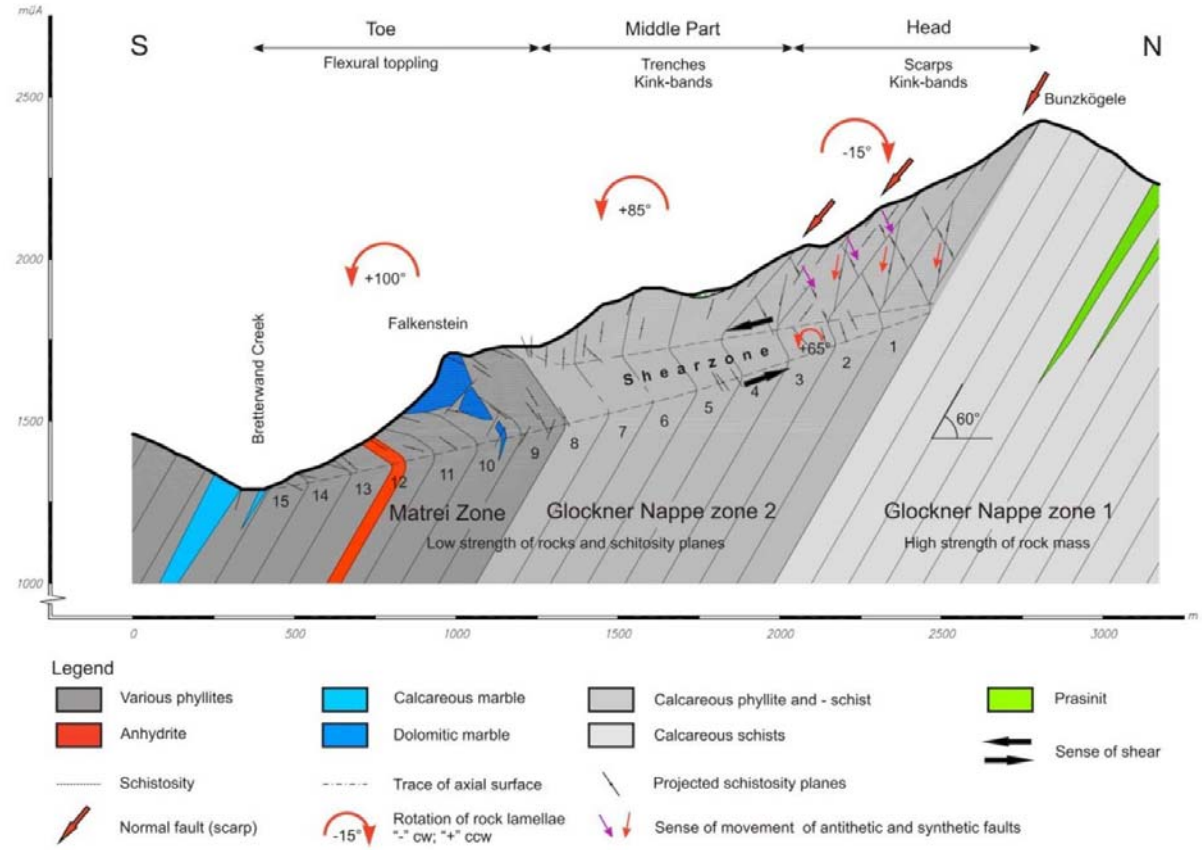

Figure 8. Cross section of the mass movement

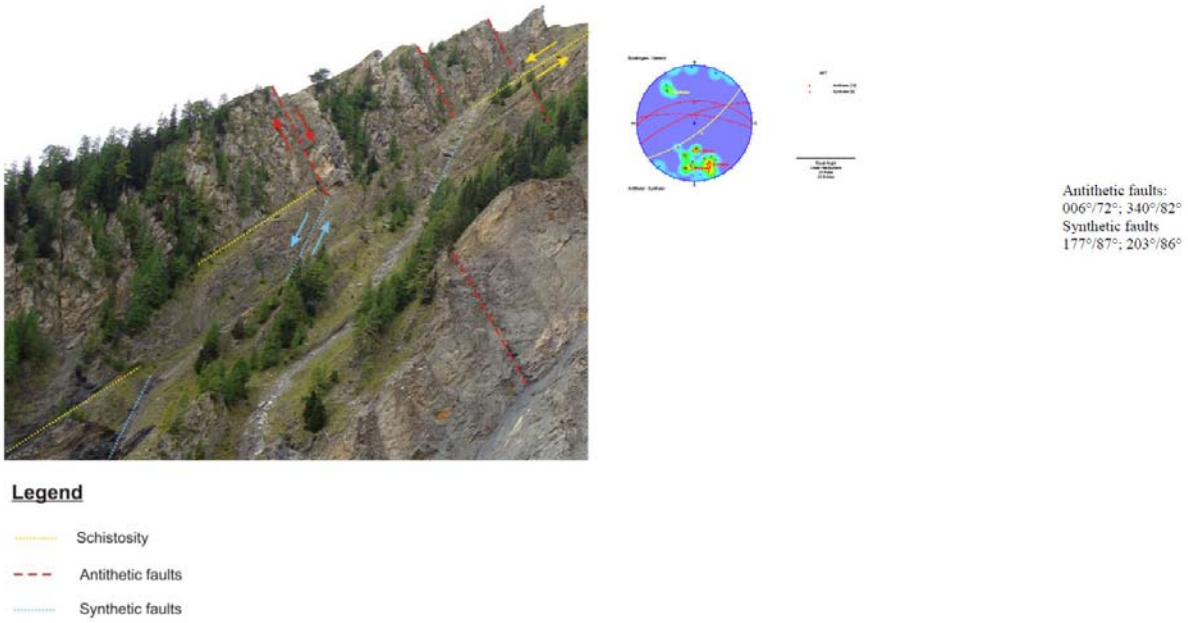

Figure 9. a) Synthetic- and antithetic faults b) Contour plot of antithetic and synthetic faults (stereographic projection of poles and great circles)

Within the above described kink-band fold the material is heavily sheared and folded by chevron type folds (Fig. 10.) The hinges of these folds, which show a characteristic kink, are broken (Fig.10b). Plastic deformation of the rock mass results from the deflection of the vectors of movement within the kink-band zone. Therefore it represents a zone of shear in a simple shear modus (black arrows in Fig. 8). The shear zone has a traingular shape, which has its origin at the deepest normal fault in the north (lamellae no. 1) and from there increases in width to the south (lamellae no. 8) with every additional slip fault.

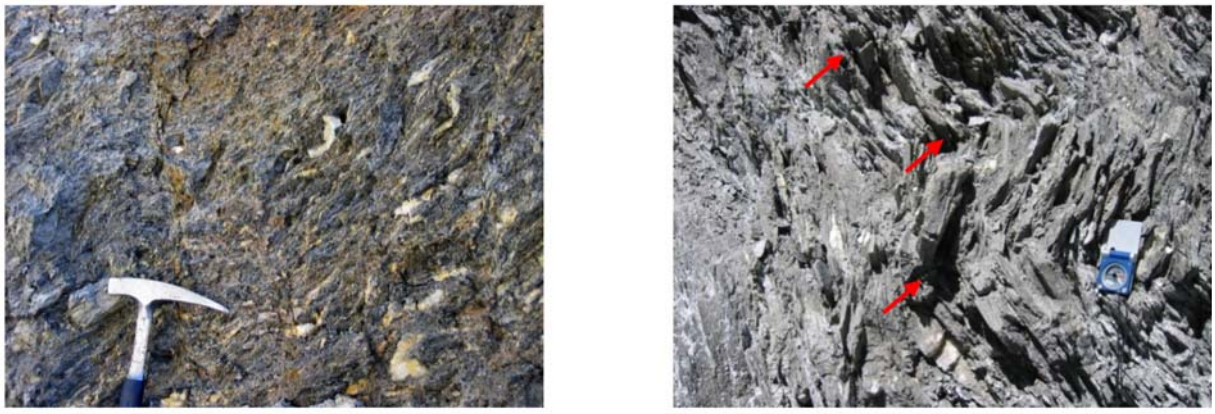

Figure 10. Character of the kink-band zone, respectively the shear zone a) heavily sheared material b) chevron folds with distinct dilatancy in the hinge zones (marked by red arrows)

The shearing and folding within the kink-band-fold is accompanied by large dilatancy of the rock mass. It can be calculated by the comparison of the volume of the deformed rock lamellae with the undeformed one (Fig. 11). This gives a value of 10%, composed by sliding along the planes of schitosity and breaking of intact rock.

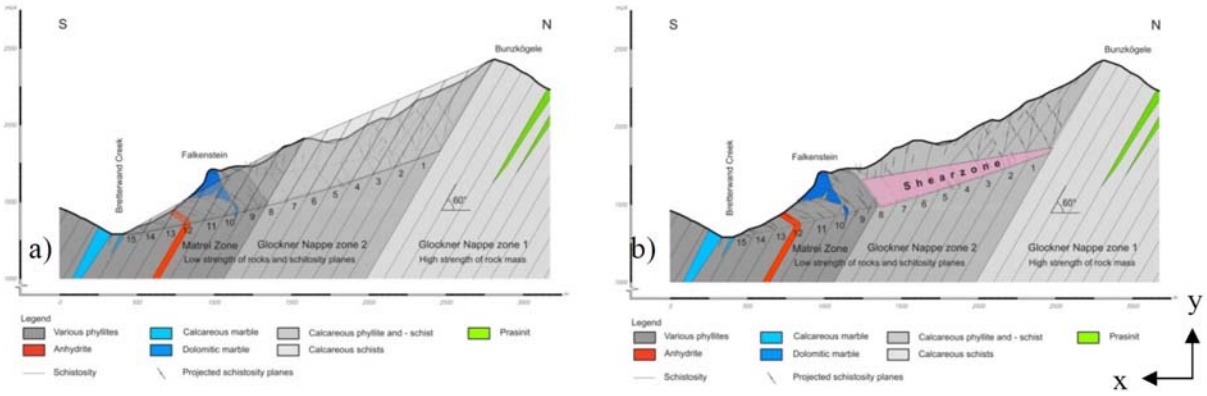

Figure 11. Calculation of rock mass dilatancy a) undeformed paleoslope b) deformed slope with shear zone

Numeric Modelling of the failure mechanism

To model the landslide's failure mechanism with a numeric program it was important to take into account the rock specific anisotropy, which is represented by the planes of schistosity. Therefore a discontinuum approach was used. The numeric program UDEC (Universal Distinct Element Code) from Itasca Consulting Group satisfies the discontinuum character of the problem.

Theory and Background

UDEC is a distinct element program. It treats the problem as an assemblage of discrete blocks, which are separated by joints. The calculation cycle alternates between a force displacement law to handle the interaction of the blocks during movement and Newton´s second law of motion to provide the displacements. Deformable blocks are subdivided by constant strain elements forming a grid. New stresses therein are calculated by employing several available material constitutive laws (ITASCA 2004).

Model geometry

The geometry for the slope was found by a restoration of the paleoslope, which is the undeformed state of the rock lamellae (Fig. 11a). This has been done by rotating back the lamellae and restoring the displacements along the normal faults. The basic block thus found was subdivided by the 60° dipping schistosity planes in parallel rock lamellae of 100 m width. In order to model the deformability of the lamellae, they were discretized into deformable triangle finite-difference zones. To improve plasticity analyses, diagonally opposed triangle zones have been applied for the greater part of the model (ITASCA 2004). For the remaining blocks common triangle zones were assigned (Fig.12).

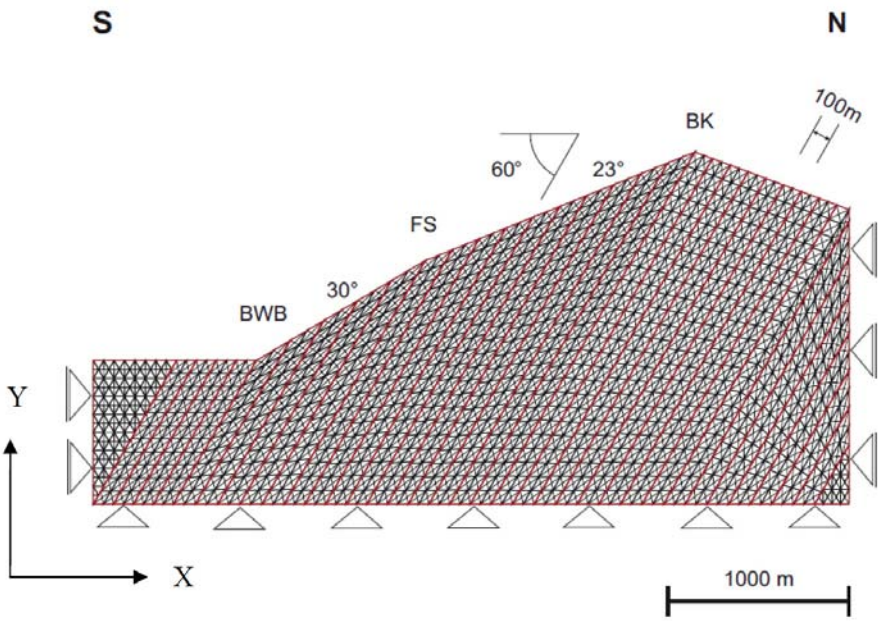

Figure 12. UDEC model. BWB. Bretterwand Creek; FS. Falkenstein; BK. Bunzkoegele

Choice of the Constitutive Model

In the study the Mohr-Coulomb material model was chosen for the Rock. The model provides a linear representation of a Mohr-Coulomb failure criterion, which is predominately a shear yield function. In the tension region the criterion is cut off by a given value. In the elastic range an isotropic material behaviour is assumed. To model the behaviour of the joints the Coulomb-slip model was applied. Sliding along the joints and opening/closure of discontinuities is principally controlled by the joint normal and joint shear stiffness (STEAD ET AL. 2001).

Both models include linear-elastic perfect-plastic behaviour. In case of yielding a non-associated shear flow rule and an associated tensile flow rule has been assigned. The default value used for the dilation angle ψ was zero.

Modelling procedure

The in situ stresses were calculated based on pure elastic material behavior. Therefore the strength parameters of rock and joints were set to high values, which prevented plastic deformations from occurring. Proper behaviour indicates equilibrium, which means that the unbalanced force and velocities converge to zero. The onset of failure, i.e. the state of limit equilibrium, was determined by using the shear strength reduction technique (Brown & King 1966, Zienkiewicz et. al. 1975, Dawson et. al. 1999) based on the definition on safety by FELLENIUS (1927).

The described failure mode was found applying the following parameters:

Table 2. Material parameters:

ρ [kg/m³]	E_m [GPa]	ν_m [-]	c_m [kPa]	ϕ_m [°]	$\sigma_{t,m}$ [kPa]
2700	6,25	0,25	200	20	10

Table 3. Joint parameters:

c_j [kPa]	ϕ_j [°]	$\sigma_{t,j}$ [kPa]
0	8	0

Results and discussion

The low strength of the parameters reflects the geomechanical properties of the described rock sequence. In accordance with observations in the field, where the schistosity planes represent smooth and clean discontinuities of high persistence, their strength is solely defined by the friction angle. The cohesion and tensile strength was therefore set to zero. The very small friction angle in Table 3 is explained by the occurrence of graphitic phyllites, which have extremely smooth surfaces.

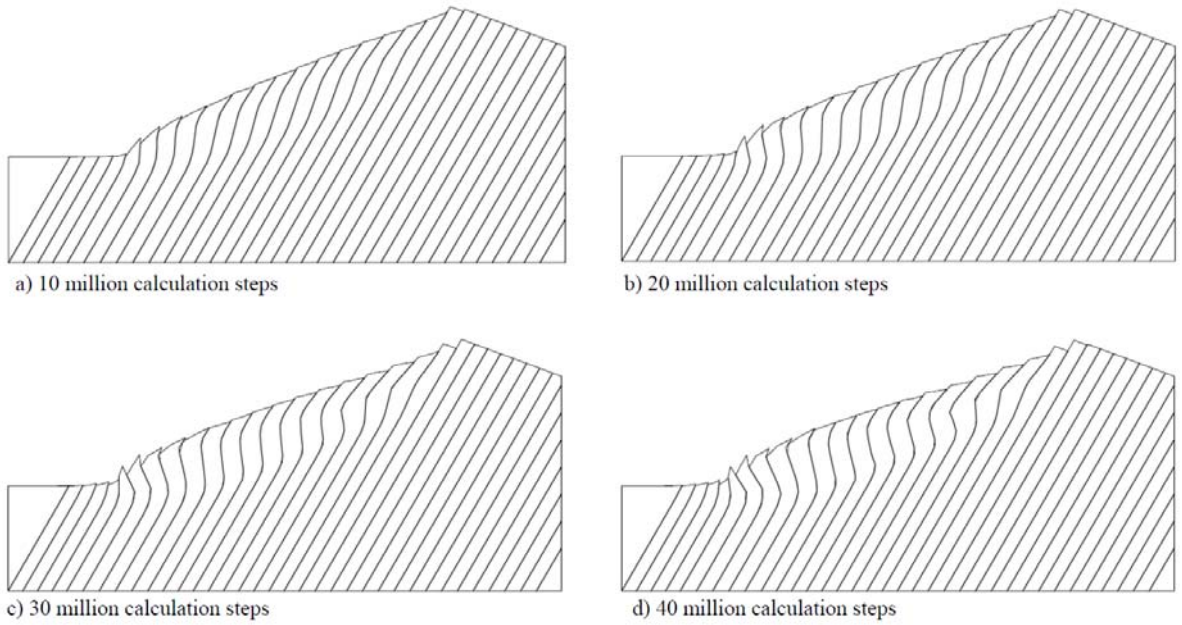

Figure 13. The figure shows different phases of the slope failure modelled by UDEC. The development of the S-structure of the rock lamellae, in the upper and middle part of the slope, is clearly shown. The toe area is characterised by flexural toppling.

Fig. 13 shows different phases of the slope failure modelled by UDEC. The development of the S-structure of the rock lamellae, in the upper and middle part of the slope, is clearly shown. The toe area is characterised by flexural toppling.

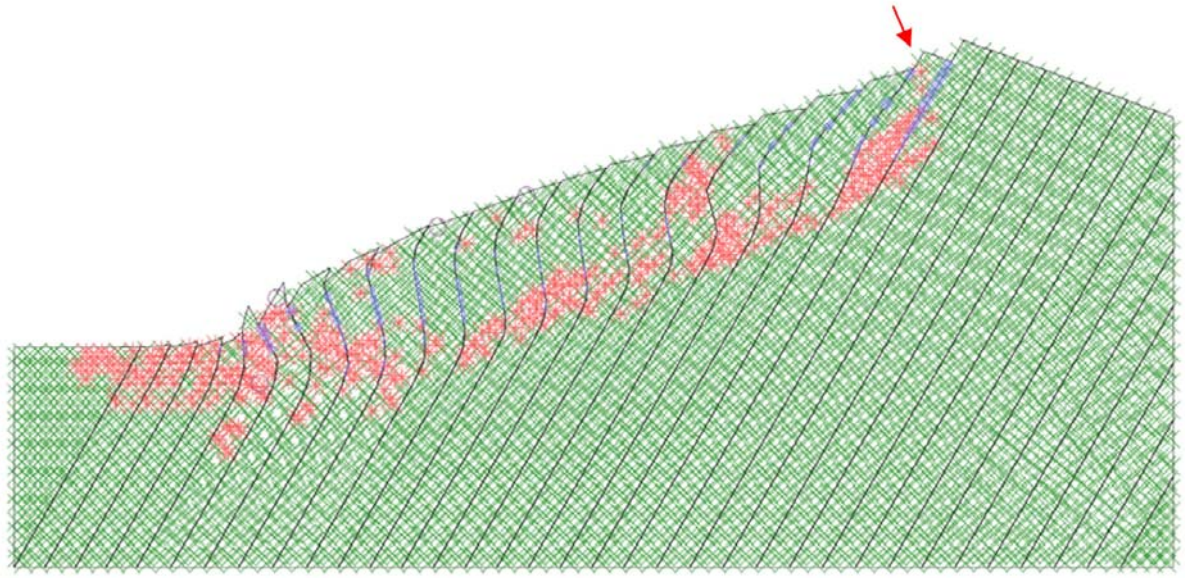

Figure 14. Plastification (shear failure red crosses; tensile failure purple circles) and shear displacements along schistosity planes (blue crosses)

The mode of failure includes large displacements along joints and the development of a broad plastic zone (Fig.14). Failure is initiated by normal faulting along the planes of weakness, which are the schistosity planes. While sliding along the schistosity planes is taking place, the rock within the zone of the kink-bands and the flexural toppling fails. This explains the absence of a distinct basal sliding surface at the bottom of the moving mass. Yielding of rock and joints is mainly shear failure. The displacement vectors in the upper part of the landslide are orientated parallel to the dip of the rock lamellae (Fig. 15). Therefore no tensile failure can be recognised here, which would be a characteristic feature of a creeping slope (ZIENKIEWICZ ET AL. 1975, POISEL & PREH 2004). On the other hand the velocity distribution corresponds to slope creep. Hence the slope may be regarded as slope creep, which is decisively controlled by the rock mass anisotropy. UDEC is not able to generate new joints like the described antithetic faults. The existence of these in the numeric calculations is indicated by locations of shear yielding in rows (red arrow Fig. 14).

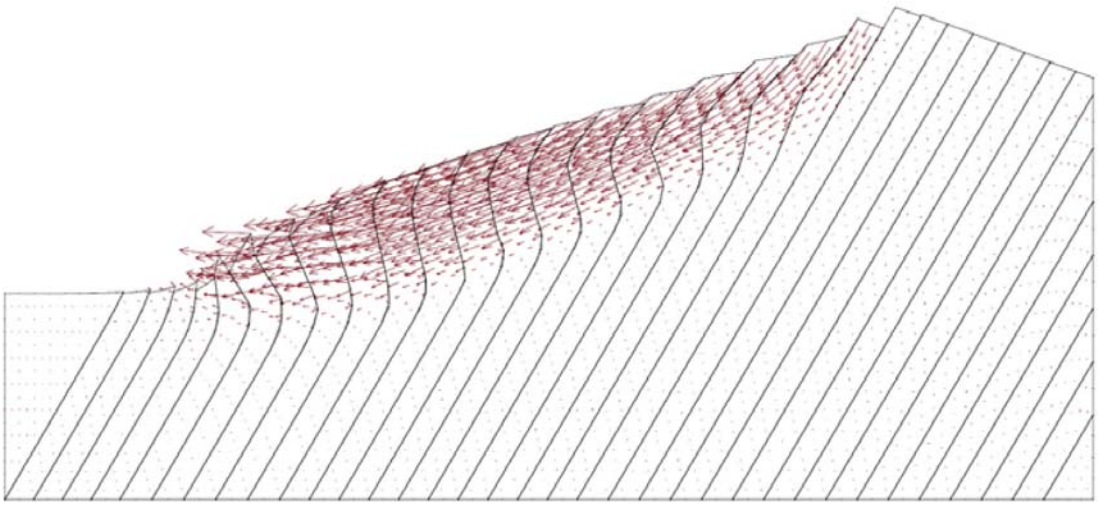

Figure 15. Displacement vectors

Conclusions

The modelled failure mechanism with UDEC displays the observed deformation pattern in the field. Slope failure is a combination of sliding along joints and breaking of rock. In the kink-band zone and the zone of flexural toppling the rock undergoes plastic deformation. Therefore no distinct basic shear zone is developed. With reference to ZISCHINSKY (1966, 1969), who idealised the slope by a continuum, one has to say that a continuum approach is not able to perform the mechanic behaviour of the slope failure. Only treatment of the problem as a discontinuum, where sliding along joints and yielding of rock individually is possible, can explain the described slope failure.

References:

Clar, E. (1963): Gefüge und Verhalten von Felskörpern in geologischer Sicht. Felsmechanik und Ingenieurgeologie, II/1, S. 4-15

Clar, E.; Weiss, P. (1965): Erfahrungen im Talzuschub des Magnesit-Bergbaues auf der Millstätter Alpe. Berg und Hüttenmänn. Monatshfte. 110, S. 447-460

Fellenius, W. (1948): Erdstatische Berechnungen mit Reibung und Kohäsion (Adhäsion) unter Annahme kreiszylindrischer Gleitflächen. Berlin

Frank, W.; Höck, V; Miller, Ch. (1987): Metamorphic and Tectonic History of the Central Tauern Window. In: Flügel, H.W.; Faupl, W. (eds.). Geodynamic of the Eastern Alps. Deuticke, Wien , pp.34-54

Cornelius, H.P.; Clar, E. (1939): Geologie des Großglocknergebietes (I. Teil). Abh. Reichsst. Bodenforsch. Zweigst. Wien, 25 , S.305

ISRM - International Society of Rock Mechanics (1981a): Suggested Methods for Quantitative Description of Discontinuities in Rock Masses (Brown, E.T. ed.) Pergamon Press, Oxford

ISRM - International Society of Rock Mechanics (1981b): Rock Characterization, Testing and Monitoring; ISRM Suggested Method. Pergamon Press, Oxford

Itasca Consulting Group (2004): UDEC (Universal Distinct Element Code) Version 4.0. MN, Minneapolis

Lammerer, B.; Weger, M. (1998): Footwall uplift in an orgenic wedge; the Tauern Window in the Eastern Alps of Europe. Tectonophysics 285, pp. 213-230

Pestal, G.; Hejl, E.; Braunstingl, R.; Schuster, R. (2009): Erläuterungen zur Geologischen Karte von Salzburg. Geol. B.-A., Wien

Mandl, G. (1988): Mechanics of tectonic faulting, models and basic concepts. Amsterdam: Elsevier

Marinos, P.; Hoek, E. (2001): Estimating the geotechnical properties of heterogeneous rock masses such as flysch. Int. Assoc. of Engng. Geologists

Poisel, R.; Preh, A. (2004): Rock slope initial failure mechanisms and their mechanical models. Felsbau 22. No. 2, pp. 40-45

Staub, R. (1924): Der Bau der Alpen. Beitr. Geol. Kt. Schweiz 52, S. 272

Stead, D.; Eberhardt, E.; Coggan, J.; Benko B. (2001): Advanced numerical techniques in rock slope stability analysis – applications and limitations. In: Kühne, M.; Einstein, H.H.; Krauter, E.; Klapperich, H.; Pöttler, R. (eds.): International Conference on Landslides-Causes, Impacts and Countermeasures. Davos, pp. 615-624

Selverstone, J. (1988): Evidence of east-west crustal extension in the Eastern Alps: Implications for the unroofing history of the Tauern window, Eastern Alps. Journal of metamorphic Petrology 7, pp. 87-105

Zienkiewicz, O. C., Humpheson, C. & Lewis, R. W. (1975). Associated and non-associated viscoplasticity and plasticity in soil mechanics. Geotechnique 25, No. 4, pp. 671-689.

Zischinsky, U. (1969): Über Sackungen. Rock Mechanics 1, S. 30-52

Zischinsky, U. (1966): On the deformation of high slopes. Proceedings of the 1st intern. Congress, Ges. Felsmechanik 2, pp. 179-185